

End Cover for Initial Value Problem: Complete Validated Algorithms with Complexity Analysis

Bingwei Zhang*

The Courant Institute of Mathematical Sciences
New York, USA
bz2517@nyu.edu

Chee Yap*[†]

The Courant Institute of Mathematical Sciences
New York, USA
yap@cs.nyu.edu

Abstract

We consider the first order autonomous differential equation (ODE) $\mathbf{x}' = \mathbf{f}(\mathbf{x})$ where $\mathbf{f} : \mathbb{R}^n \rightarrow \mathbb{R}^n$ is locally Lipschitz. For a box $B_0 \subseteq \mathbb{R}^n$ and $h > 0$, the set of solutions $\mathbf{x} : [0, h] \rightarrow \mathbb{R}^n$ that satisfies $\mathbf{x}'(t) = \mathbf{f}(\mathbf{x}(t))$ and $\mathbf{x}(0) \in B_0$ is denoted $\text{IVP}_f(B_0, h)$. We provide a complete validated algorithm for the following **End Cover Problem**: given (f, B_0, ε, h) , to compute a finite set C of boxes such that

$$\text{End}_f(B_0, h) \subseteq \bigcup_{B \in C} B \subseteq \left(\text{End}_f(B_0, h) \oplus [-\varepsilon, \varepsilon]^n \right)$$

where $\text{End}_f(B_0, h) = \{\mathbf{x}(h) : \mathbf{x} \in \text{IVP}(B_0, h)\}$. We will also give a complexity analysis of our algorithm, and introduce an alternative technique to compute End Cover C based on covering the boundary of $\text{End}_f(B_0, h)$. Finally, we give experimental results indicating the practicality of our techniques.

Keywords

initial value problem, IVP, end cover problem, reachability problem, end enclosure problem, validated algorithms, interval methods, logarithmic norm, matrix measure,

ACM Reference Format:

Bingwei Zhang and Chee Yap. 2026. End Cover for Initial Value Problem: Complete Validated Algorithms with Complexity Analysis. In . ACM, New York, NY, USA, 14 pages. <https://doi.org/XXXXXXX.XXXXXXX>

1 Introduction

The initial value problem (IVP) for ordinary differential equations leads to challenging computational problems. A chief reason is that approximation errors typically grow exponentially large with time. So simulating an IVP over a long time span will break down. Other difficulties include the presence of singularities as well as the phenomenon of stiffness (regions where the solution changes quickly). Although numerical algorithms based on machine precision are very successful in practice, they are often qualitatively wrong. So

*Both authors contributed equally to this research.

[†]Corresponding author

The results of this research was funded by NSF Grant #CCF-2212462.

Permission to make digital or hard copies of all or part of this work for personal or classroom use is granted without fee provided that copies are not made or distributed for profit or commercial advantage and that copies bear this notice and the full citation on the first page. Copyrights for components of this work owned by others than the author(s) must be honored. Abstracting with credit is permitted. To copy otherwise, or republish, to post on servers or to redistribute to lists, requires prior specific permission and/or a fee. Request permissions from permissions@acm.org.

Conference'17, Washington, DC, USA

© 2026 Copyright held by the owner/author(s). Publication rights licensed to ACM.
ACM ISBN 978-1-4503-XXXX-X/2018/06
<https://doi.org/XXXXXXX.XXXXXXX>

there remains a need for certifiable or **validated algorithms**. Validated IVP algorithms have been studied from the beginning of interval analysis over 50 years ago [12]. Unfortunately, current validated IVP algorithms are only **partially correct** in the sense that, if they halt, then the output is validated [23]. But halting is rarely addressed. Thus the challenge is to construct **complete validated algorithms**, i.e., halting ones.

In this paper, we consider the following system of first order ordinary differential equations (ODEs)

$$\mathbf{x}' = \mathbf{f}(\mathbf{x}) \quad (1)$$

where $\mathbf{f} = (f_1, \dots, f_n) : \mathbb{R}^n \rightarrow \mathbb{R}^n$ is locally Lipschitz. For $B_0 \subseteq \mathbb{R}^n$ and $h > 0$, let $\text{IVP}_f(B_0, h)$ denote the set of total differentiable functions $\mathbf{x} = (x_1, \dots, x_n) : [0, h] \rightarrow \mathbb{R}^n$ such that $\mathbf{x}(0) \in B_0$ and the time derivative $\mathbf{x}' = (x'_1, \dots, x'_n)$ satisfies (1). Call each $\mathbf{x} \in \text{IVP}_f(B_0, h)$ a **solution** to the **IVP instance** (f, B_0, h) or¹ (B_0, h) . The **end slice** and **image** of $\text{IVP}_f(B_0, h)$ are

$$\begin{aligned} \text{End}_f(B_0, h) &:= \{\mathbf{x}(h) : \mathbf{x} \in \text{IVP}_f(B_0, h)\} \\ \text{Image}_f(B_0, h) &:= \{\mathbf{x}(t) : \mathbf{x} \in \text{IVP}_f(B_0, h), t \in [0, h]\} \end{aligned} \quad (2)$$

If B_1 contains $\text{End}_f(B_0, h)$ (resp., $\text{Image}_f(B_0, h)$), we call B_1 an **end enclosure** (resp., **full enclosure**) of $\text{IVP}_f(B_0, h)$. In our previous paper [23], we gave a complete validated algorithm for the **End Enclosure Problem**² which is defined by this header:

END ENCLOSURE PROBLEM:

$$\text{EndEnc}_f(B_0, \varepsilon, \mathbf{p}_0, h) \rightarrow (\underline{B}_0, \bar{B}_1)$$

INPUT: $B_0 \in \square\mathbb{R}^n$, $\varepsilon > 0$, $\mathbf{p}_0 \in B_0$, $h > 0$ where (B_0, h) is valid.

The optional arguments default to $h = 1$, $\mathbf{p}_0 = m(B_0)$.

OUTPUT: $\underline{B}_0, \bar{B}_1 \in \square\mathbb{R}^n$ such that

$$\mathbf{p}_0 \in \underline{B}_0 \subseteq B_0, \text{End}_f(\underline{B}_0, h) \subseteq \bar{B}_1 \in \square\mathbb{R}^n, \text{ and max width } w_{\max}(\bar{B}_1) < \varepsilon. \quad (3)$$

Here, $\square\mathbb{R}^n$ denotes the set of compact boxes in \mathbb{R}^n , and our algorithms assume that the B 's in input and output are boxes. The usual IVP formulation in the literature assumes the singleton $B_0 = \{\mathbf{p}_0\}$. Our formulation with a box B_0 (following Corliss [4, Section 3]) is more realistic since, in real applications (e.g. biology or physics), one never knows an exact point \mathbf{p}_0 , only a range of interest.

A key insight for proving halting of our algorithm is to formulate Problem (3) as a *promise problem*: the input (B_0, h) is promised to be

¹Note that we often omit \mathbf{f} , as it is usually fixed or implicit in a given context.

²Computational problems are specified using a header of the form

$$\text{PROBLEM}(\mathbf{a}; \mathbf{b}) \rightarrow \mathbf{c}$$

where $\mathbf{a}, \mathbf{b}, \mathbf{c}$ are sequences representing (respectively) the required arguments, the optional arguments, and the outputs. Default values for optional arguments may be directly specified (as in $h = 1$ above) or they may be context dependent. In [23], \mathbf{p}_0 was implicitly defaulted to the midpoint of B_0 .

valid. This means that, for all $p_0 \in B_0$, the ODE (1) has³ a unique solution $x : [0, h] \rightarrow \mathbb{R}^n$ with $x(0) = p_0$.

The output requirement $w(\bar{B}_1) < \varepsilon$ implies that B_0 must be allowed to shrink to some \underline{B}_0 (while keeping $p_0 \in \underline{B}_0$). In this paper, we address a stronger variant in which shrinkage of B_0 is not allowed. This is the **End Cover Problem** defined by this header:

END COVER PROBLEM:
 $\text{EndCover}_f(B_0, \varepsilon; h = 1) \rightarrow C$

INPUT: $B_0 \in \square \mathbb{R}^n$, $\varepsilon > 0$, $h > 0$ where (B_0, h) is valid.
 OUTPUT: C is an ε -cover of $\text{End}_f(B_0, h)$.
 I.e., C is a finite set of boxes such that
 $\text{End}_f(B_0, h) \subseteq \bigcup C \subseteq (\text{End}_f(B_0, h) \oplus [\pm\varepsilon]^n)$

(4)

Here, $[\pm\varepsilon]^n$ denotes the box $\prod_{i=1}^n [-\varepsilon, \varepsilon]$, $A \oplus B$ is the Minkowski sum of sets $A, B \subseteq \mathbb{R}^n$, and $\bigcup C := \bigcup_{B \in C} B$ is a subset of \mathbb{R}^n . For any $\varepsilon > 0$, clearly ε -covers of $\text{End}_f(B_0, h)$ exists. Our introduction of a *a priori* ε -bounds in the problems (3) and (4) is clearly highly desirable. As far as we know, current IVP algorithms do not offer such ε guarantees.

1.1 What is new in this paper

We have three main objectives: The first is to enhance our end enclosure algorithm in [23], leading to a solution for the End Cover Problem (4). The issue is this: suppose we want to compute an ε -cover for the IVP instance (B_0, ε, h) where $B_0 = [a, b]$ ($n = 1$). Using our End Enclosure Algorithm, we can compute B_1 that is an ε -cover of $\text{End}_f([a, a_1], h)$ for some $a < a_1 \leq b$. If $a_1 < b$, then we repeat this process to compute a B_2 to cover $\text{End}_f([a_1, a_2], h)$ for some $a_1 < a_2 \leq b$, etc. If this process terminates, we have a finite ε -cover $C = \{B_1, B_2, \dots\}$. Viewing x as space variables, this shows that our new problem amounts to computing a “space cover” of $[a, b]$, analogous to the “time cover” of $[0, h]$ in the original End Enclosure Problem.

In Figure 1, we show the output of our end cover algorithm on the Volterra-Lotka (or predator-prey) system (Table 1, Section 5) with $\varepsilon = 0.1$. We show five IVP instances ($i = 0, \dots, 4$)

$$(f, B_0, h_i, \varepsilon) = \left(\left[\begin{array}{c} 2x(1-y) \\ -y(1-x) \end{array} \right], \text{Box}_{(1,3)}(0.1), h_i, 0.1 \right)$$

where $h_i \in (0, 0.1, 0.4, 0.7, 1.0)$ and $\text{Box}_p(w)$ denotes box $p + [-w, w]^2$.

Our second objective is to introduce an alternative approach to computing end covers: the idea is to reduce the covering of $\text{End}_f(B_0, h)$ to the covering of its boundary, $\partial(\text{End}_f(B_0, h))$. Any ε -cover of $\partial(\text{End}_f(B_0, h))$ is called an **ε -boundary cover** of $\text{End}_f(B_0, h)$. Thus we reduce the n -dimensional problem to a $(n-1)$ -dimensional one, modulo a **filler problem**: given C , an ε -boundary cover of $\text{End}_f(B_0, h)$, to compute a finite set of boxes C_0 so that $C \cup C_0$ is an ε -cover of $\text{End}_f(B_0, h)$. Intuitively, C_0 covers the “interior” of $\bigcup C$.

In Figure 2, we run our boundary cover algorithm on the same Volterra-Lotka instances of Figure 1, but with $\varepsilon = 0.01$ instead of $\varepsilon = 0.1$. The running time is much faster than that of the end cover algorithm. The filler problem to convert C_i into an end cover of

³Without such a promise, the algorithm would be required to output “invalid” when no solution exists. This would a *fortiori* decide validity of the input, a decision problem that remains open [23].

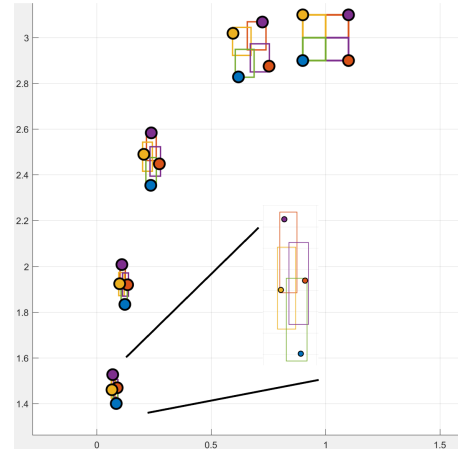


Figure 1: ε -End Covers ($\varepsilon = 0.1$) at times $h_i \in (0, 0.1, 0.4, 0.7, 1.0)$ for $i = 0, \dots, 4$. The boxes in C are colored for visualization. An enlarged image for the cover at $h_4 = 1.0$ is also shown.

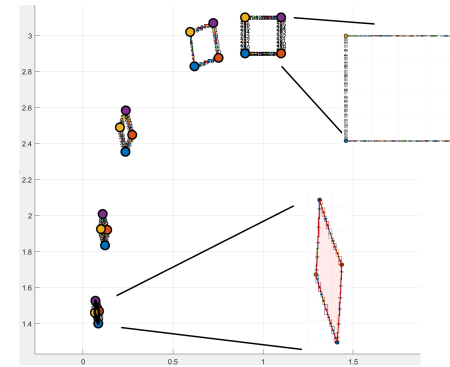


Figure 2: ε -Boundary Covers ($\varepsilon = 0.01$) at times $h_i \in (0, 0.1, 0.4, 0.7, 1.0)$ for $i = 0, \dots, 4$. The boxes in a cover C are colored to visualize them. An enlarged image for the cover at $h_4 = 1.0$ is also shown.

$\text{End}_f(B_0, h_i)$ is relatively easy for these instances because the “interior polygon” (pink area in the enlarged image) of C_i are simple polygons. We reduced ε to 0.01 (from the previous 0.1) to ensure the interior polygons are non-empty. Despite the smaller ε , the boundary computation is much faster than the end cover computation.

Although the boundary method seems like a natural suggestion, its justification depends on a non-trivial result⁴ called the **Invariance of Domain Theorem** from L.E.J. Brouwer.

We use this result to prove Section 3 that if B_0 is homeomorphic to a ball (e.g., a box), then $\text{End}_f(B_0, h)$ is also homeomorphic to a ball. So, if C is an ε -boundary enclosure of $\text{End}_f(B_0, h)$, then $\bigcup C$ is a connected set which can be “filled” by a set C_0 of boxes to give an ε -end cover, as noted above.

Our third objective is to give a complexity analysis of our end cover algorithm. Note that complexity analysis is rarely attempted

⁴See [Terry Tao’s blog](#) on Brouwer’s Fixed Point Theorem.

in the validated algorithms literature for various reasons. Using the enhanced End Enclosure algorithm (Section 2.3) we can now give explicit bounds, based on implicit parameters which can be derived from the actual inputs.

1.2 Brief Literature Review and Background.

For the validated IVP literature, we refer to the surveys by Corliss [4], Nedialkov et al. [13], and other references in [23]. The computational problems associated with $\text{End}(B_0)$ have many applications, and are often called **reachability problems** in non-linear control and verification (e.g., [5, 16]). The notions of partially correct algorithms and promise problems are standard in theoretical computer science. Partial correctness is useful since we can now split correctness into separate concerns: halting and correct output. Promise problems [6] are also natural in numerical computation, where typical promises assert non-singularity or good conditioning. Algorithms for promise problems may assume the promised condition without checking it.

Ultimately, validated algorithms require arbitrary-precision numerics (e.g., big-number packages such as `gmp`). Although this is our goal, we avoid a direct discussion of this aspect in order to focus on the main algorithmic development. Following standard practice, we describe an **abstract algorithm** A that operates on exact mathematical objects. But such abstract descriptions must ultimately be replaced by implementable operations. Following [21], this is done in two steps: first, A is transformed into its **interval version** $\Box A$, which computes with bounding intervals. Since $\Box A$ is still abstract (e.g., the interval bounds may involve real numbers), we need to convert $\Box A$ to an **effective version** $\tilde{\Box} A$, that uses only implementable operations (e.g., `bigFloats`) and finite representations. Once A is given (as in this paper), the transformations $A \rightarrow \Box A \rightarrow \tilde{\Box} A$ are usually straightforward, as global properties are largely preserved. This Abstract/Interval/Effective approach is outlined in [21]. However, not every abstract algorithm A admits a simple interval version $\Box A$. The difficulty arises when A relies on a “zero problem” (see [22]). For example, Gaussian elimination for computing determinants relies on knowing that a pivot is non-zero, and so no simple $\Box A$ exists. Our IVP algorithms avoid such zero problems.

Our notion of trajectory bundles in Subsection 3.1 appears to be new; but the term has appeared in contexts such as in path planning, optimization and optics. But these refer to the algorithmic technique of “multiple shooting or trajectory sampling” to better estimate the end set. E.g., [1, 18].

1.3 Paper Overview.

The remaining sections of this paper are as follows: In Section 2, we first establish some notations and review our previous End Enclosure algorithm. Then we describe a modification to enhance its performance. This enhanced algorithm is used to construct our End Cover Algorithm. In Section 3, we introduce the Boundary Cover Problem. We prove a key result based on Brouwer’s Invariance Theorem algorithm that reduces it to End Covers in one lower dimension. In Section 4, we analyze the complexity of the End Cover Algorithm in Sections 2. In Section 5, we describe compare our implementation of the End Cover algorithms, comparing them

with two well-known validated IVP algorithms (CAPD and VNODE). We conclude in Section 6 and include an Appendix for proofs. We show more experiments on Appendix B.

The present paper is self-contained. But in [24], we provided more experimental results and other elaborations. This pdf file contain hyperlinks for references, theorems, etc.

2 The End Cover Problem

This section will describe an enhancement of the `EndEnc1` Algorithm in [23]. We then use the enhanced version as a subroutine to solve End Cover Problem. The enhancement is also needed for its complexity analysis. But first, we establish some notations.

2.1 Notations and Basic Concepts

We collect the basic terminology here for easy reference, largely following [23]. We use bold font like $\mathbf{p} = (p_1, \dots, p_n)$ for vectors, with $(\mathbf{p})_i = p_i$ as the i th coordinate function. The origin in \mathbb{R}^n is denoted $\mathbf{0} = (0, \dots, 0)$. Let $\Box\mathbb{R}$ denote the set of compact intervals. We identify the interval $[a, a]$ with $a \in \mathbb{R}$ and thus $\mathbb{R} \subseteq \Box\mathbb{R}$. For $n \geq 1$, let $\Box\mathbb{R}^n := (\Box\mathbb{R})^n$ denote the set of (axes-aligned) boxes in \mathbb{R}^n . For a non-empty set $S \subseteq \mathbb{R}^n$, let $\text{Ball}(S)$ and $\text{Box}(S)$ denote, respectively, the smallest ball and smallest box containing S . Also, let $\mathbf{m}(S)$ denote the midpoint of $\text{Box}(S)$. For $\alpha \geq 0$, the α -dilation operator is $\alpha S := \{\alpha \mathbf{p} : \mathbf{p} \in S\}$. E.g., if $n = 1$ and $S = [2, 6]$ then $\frac{1}{2}S = [1, 3]$.

The *Box* and *Ball* operators in \mathbb{R}^n can also take numerical parameters: $\text{Ball}(r)$ is the ball in \mathbb{R}^n centered at $\mathbf{0}$ of radius $r \geq 0$, and $\text{Box}(\mathbf{r}) := \prod_{i=1}^n [-r_i, r_i]$ where $\mathbf{r} = (r_1, \dots, r_n) \geq \mathbf{0}$. If $\mathbf{p} \in \mathbb{R}^n$, let $\text{Ball}_{\mathbf{p}}(\mathbf{r}) := \mathbf{p} + \text{Ball}(\mathbf{r})$ and $\text{Box}_{\mathbf{p}}(\mathbf{r}) := \mathbf{p} + \text{Box}(\mathbf{r})$. Simply write $\text{Box}(\mathbf{r})$ and $\text{Box}_{\mathbf{p}}(\mathbf{r})$ if $r_i = r$ for all $i = 1, \dots, n$. The **width** of the box $B = \text{Box}_{\mathbf{p}}(\mathbf{r})$ is $\mathbf{w}(B) := 2\mathbf{r}$. The dimension of $B \in \Box\mathbb{R}^n$ is the number $\dim(B) \in \{0, \dots, n\}$ of positive values in $\mathbf{w}(B)$. The **maximum, minimum widths** of B are $w_{\max}(B) := \max_{i=1}^n (\mathbf{w}(B))_i$, and similarly for $w_{\min}(B)$. The natural extension of any function $f : X \rightarrow Y$ is used throughout; this extension (still denoted f) is $f : 2^X \rightarrow 2^Y$ where $f(X) = \{f(x) : x \in X\}$ and 2^X is the power set of X . If $f : \mathbb{R}^n \rightarrow \mathbb{R}^m$, then a **box function** for f is any function of the form $\Box f : \Box\mathbb{R}^n \rightarrow \Box\mathbb{R}^m$ that is conservative, i.e., $f(B) \subseteq \Box f(B)$, and convergent, i.e., $\mathbf{p} = \lim_{i \rightarrow \infty} B_i$ implies $f(\mathbf{p}) = \lim_{i \rightarrow \infty} \Box f(B_i)$. For simplicity, we often say “compute $f(B)$ ” but we actually compute $\Box f(B)$ using interval methods.

Normalized Taylor Coefficients: Although IVP theory only requires the function f in (1) to be locally Lipschitz, practical algorithms need f to be C^k for moderately large k . Following [10], we assume $k = 20$ (a global constant) in our implementations. For $i = 0, \dots, k$, the i th **normalized Taylor coefficient** of f is recursively defined by $f^{[0]}(x) = x$ and for $i \geq 1$, $f^{[i+1]}(x) = \frac{1}{i} \left(J_{f^{[i-1]}} \bullet f \right)(x)$ where J_g is the Jacobian of any $g = g(x) \in C^1(\mathbb{R}^n \rightarrow \mathbb{R}^n)$. E.g., $f^{[1]} = f$ and $f^{[2]}(x) = \frac{1}{2} (J_f \bullet f)(x)$. The order k Taylor expansion of $f(x)$ at the point $t = t_0$ is

$$\begin{aligned} \mathbf{x}(t_0 + h) &= \left\{ \sum_{i=0}^{k-1} h^i f^{[i]}(\mathbf{x}(t_0)) \right\} + h^k f^{[k]}(\mathbf{x}(\xi)) \\ &\in \left\{ \sum_{i=0}^{k-1} h^i f^{[i]}(\mathbf{x}(t_0)) \right\} + h^k f^{[k]}(F) \end{aligned} \quad (5)$$

where $0 \leq \xi - t_0 \leq h$ and F is any enclosure of $\{\mathbf{x}(t) : t \in [0, h]\}$.

Since (1) is autonomous, we will normally assume that the initial time is $t = 0$. Up to time scaling, we can even make $h = 1$. So we can let h be an optional parameter with default value $h = 1$; this is mainly to simplify notations but our results hold for any $h > 0$. Recall the set $\text{IVP}_f(B_0; h)$ defined in the introduction. If $B_0 = \{\mathbf{p}_0\}$ is a singleton, we simply write $\text{IVP}_f(\mathbf{p}_0; h)$. We say $\text{IVP}_f(B_0; h)$ is **valid** if for each $\mathbf{p}_0 \in B_0$, $\text{IVP}_f(\mathbf{p}_0; h)$ is a singleton (comprising the unique and bounded solution \mathbf{x} with $\mathbf{x}(0) = \mathbf{p}_0$). Since f is usually fixed, they appear in subscripts and is often omitted, as in $\text{IVP}(B_0; h)$.

Admissibility: If F and E are (respectively) full enclosure and end enclosure of $\text{IVP}_f(B_0, h)$, then we call (B_0, h, F) an **admissible triple** and (B_0, h, F, E) an **admissible quad**. We simply say “admissible” when it is clearly triple or quad.

For closed convex sets $E, F \subseteq \mathbb{R}^n$ and $h > 0$, [23, Lemma 1] says that (E, h, F) is admissible provided and $E \subseteq \text{interior}(F)$

$$\sum_{i=0}^{k-1} [0, h]^i f^{[i]}(E) + [0, h]^k f^{[k]}(F) \subseteq F. \quad (6)$$

If, in addition, we have $[0, h]^k f^{[k]}(F) \subseteq [\pm\epsilon]^n$, then we say (E, h, F) is ϵ -**admissible**

Logarithmic norms. Let $\mu_p(A)$ denote the **logarithmic norm** ($\log\text{Norm}$) of a square matrix $A \in \mathbb{C}^{n \times n}$ based on the induced matrix p -norm. For specificity, assume $p = 2$. For $f \in C^1(\mathbb{R}^n \rightarrow \mathbb{R}^n)$, the **logNorm bound** of $B \subseteq \mathbb{R}^n$ is defined as $\mu_2(J_f(B)) := \sup \{\mu_2(J_f(\mathbf{p})) : \mathbf{p} \in B\}$ where J_f is the Jacobian matrix of f .

In this paper, in addition to the convention of specifying problems as in the footnote for (3), we have a corresponding header for algorithms that solve the problem:

$$\text{ALGORITHM}(\mathbf{a}; \mathbf{b}; \mathbf{d}) \rightarrow \mathbf{c}. \quad (7)$$

This algorithm header has the problem arguments \mathbf{a}, \mathbf{b} , but might further have optional “hyperparameters” \mathbf{d} which have no effect on the correctness of the algorithm, but users can use them to provide hints that may speed up the algorithm.

2.2 Review of EndEnc1 Algorithm

Most validated IVP algorithms are based on two basic subroutines which we call **Step A** and **Step B**, with these headers:

$$\begin{array}{ll} \text{StepA}_f(E; H = 1) & \rightarrow (h, F) \\ \text{StepB}_f(E, h, F; \epsilon_0 = w_{\min}(E)) & \rightarrow E_1 \end{array} \quad (8)$$

where (E, h, F) and (E, h, F, E_1) are admissible. Note that H, ϵ_0 are optional, with the indicated default values. Starting with E_0 , we call Step A then Step B to produce an admissible quad:

$$E_0 \xrightarrow{\text{StepA}} (E_0, h_0, F_1) \xrightarrow{\text{StepB}} (E_0, h_0, F_1, E_1). \quad (9)$$

In general, by calling Step A then Step B on E_{i-1} ($i = 0, 1, \dots$), we produce the the i th **stage** represented by the admissible quad (E_{i-1}, h_i, F_i, E_i) . Iterating m times, we organize these quads into an **m -stage scaffold** data structure $\mathcal{S} = (t, E, F, G)$ where

$$\begin{array}{ll} t = (0 = t_0 < t_1 < \dots < t_m), & E = (E_0, E_1, \dots, E_m) \\ F = (F_1, \dots, F_m), & G = (G_1, \dots, G_m) \end{array} \quad (10)$$

where $t_i = t_{i-1} + h_i$ and the G_i 's is the i th **refinement substructure** used for refining the i th stage. This scaffold allows us to achieve

much stronger objectives than are possible in previous IVP algorithms.

Let \mathcal{S} be an m -stage scaffold \mathcal{S} . It is self-modified by 2 subroutines: the first is $\mathcal{S}.\text{Extend}$, which turns \mathcal{S} into a $m+1$ -stage scaffold. It is straightforward (basically calling Steps A and B), so we focus on the second subroutine $\mathcal{S}.\text{Refine}$ with this header:

$$\begin{array}{l} \mathcal{S}.\text{Refine}(\epsilon_0) \\ \text{INPUT: } m\text{-stage scaffold } \mathcal{S} \text{ and } \epsilon_0 > 0. \\ \text{OUTPUT: } \mathcal{S}' \text{ is a refinement of } \mathcal{S} \text{ that is } \epsilon_0\text{-bounded,} \\ \text{i.e., } w_{\max}(E_m) \leq \epsilon_0. \end{array} \quad (11)$$

Each iteration of the while-loop in $\mathcal{S}.\text{Refine}$ is called a **phase**. Each phase will refine the i th stage of \mathcal{S} (from $i = 1$ to $i = m$). We can visualize each phase as a row of the **phase-stage** diagram in (12):

	Stage 1	...	Stage i	...	Stage m
Phase 1:	\widehat{h}_1^1	...	\widehat{h}_i^1	...	\widehat{h}_m^1
⋮	⋮	⋮	⋮	⋮	⋮
Phase k :	\widehat{h}_1^k	...	\widehat{h}_i^k	...	\widehat{h}_m^k
⋮	⋮	⋮	⋮	⋮	⋮

(12)

Each entry of the diagram is indexed by a pair (k, i) representing the k th phase at the i th stage. The operations at (k, i) are controlled by the i th refinement substructure

$$G_i = G_i(\mathcal{S}) = ((\pi_i, \mathbf{g}_i), (\ell_i, \overline{E}_i, \overline{F}_i), (\overline{\mu}_i^1, \overline{\mu}_i^2), (\delta_i, h_i^{\text{euler}})). \quad (13)$$

Here we focus on the components in red. We call $(\ell_i, \overline{E}_i, \overline{F}_i)$ the i th **mini-scaffold** and $\ell_i \geq 0$ is the **level**. It represents a subdivision of $[t_i - t_{i-1}]$ into 2^{ℓ_i} mini-steps of size $\widehat{h}_i := (t_i - t_{i-1})2^{-\ell_i}$, and $\overline{E}_i, \overline{F}_i$ are 2^{ℓ_i} -vectors representing admissible quads $(\overline{E}_i[j-1], \widehat{h}_i, \overline{F}_i[j], \overline{E}_i[j])$ (for $j = 1, \dots, 2^{\ell_i}$). In (12), we write \widehat{h}_i^k for the value of \widehat{h}_i in phase k . At each (k, i) , we can refine the 2^{ℓ_i} admissible quads by either calling $\mathcal{S}.\text{EulerTube}(i)$ or $\mathcal{S}.\text{Bisect}(i)$. Ideally, we want to call $\mathcal{S}.\text{EulerTube}(i)$ because it is very fast. But it has a precondition, viz., \widehat{h}_i is less than h_i^{euler} in G_i (see (13)). If the precondition fails, we call $\mathcal{S}.\text{Bisect}(i)$ and also increment the level ℓ_i . This $\text{Bisect}(i)/\text{EulerTube}(i)$ design is critical for the overall performance of our algorithm (see [23, Table B]). The precondition $\widehat{h}_i < h_i^{\text{euler}}$ guarantees that the polygonal Euler path produced by Euler Tube method is guaranteed to lie in the δ_i -tube of each solution $\mathbf{x} \in \text{IVP}(E_i, t_i - t_{i-1})$ ([23, Lemma 6, Sect.2.5]). The value h_i^{euler} is computed by the function $h^{\text{euler}}(H, \overline{M}, \mu, \delta)$ in [23, Eq. (12)].

2.3 The Enhanced EndEnc1 Algorithm

The EndEnc1 algorithm itself is unchanged from [23], except that it calls the following **enhanced Refine** subroutine:

```

S.Refine( $\varepsilon_0, \mathbf{p}_0$ ) (enhanced version)
INPUT:  $m$ -stage scaffold  $S, \varepsilon_0 > 0$  and point  $\mathbf{p}_0 \in E_0(S)$ .
OUTPUT:  $S$  remains an  $m$ -stage scaffold
        that satisfies  $w_{\max}(E_m) \leq \varepsilon_0$ .
-----
 $r_0 \leftarrow w_{\max}(E_m(S))$ .
While ( $r_0 > \varepsilon_0$ )
  ▶ The original code, " $E_0(S) \leftarrow \frac{1}{2}E_0(S)$ ," is replaced by the next lines:
   $\bar{\mu} \leftarrow \max\{\bar{\mu}^1(G_i(S)) : i = 1, \dots, m\}$ .
   $\Delta \leftarrow \max_{i=1}^m \delta(G_i(S))$ 
  If ( $e^{\bar{\mu}} \Delta m < \varepsilon_0/8$  and  $e^{\bar{\mu}}(t_m(S) - t_0(S)) w_{\max}(E_0(S)) < \varepsilon_0/2$ )
    For ( $i = 1, \dots, m$ ) ◀ CONDITION 3 (20) holds
       $G_i(S).\delta \leftarrow 2G_i(S).\delta$ 
       $S.\text{EulerTube}(i)$ . ◀ Create a chain
    Return  $S$  ◀ Stop the algorithm
   $r_0 \leftarrow w_{\max}(E_m(S))$ 
  For ( $i = 1, \dots, m$ ) ◀ Begin new phase
    If ( $e^{\bar{\mu}} \delta(G_i(S)) m < \varepsilon_0/8$ ) ◀ CONDITION 2 (19) holds
      Continue ◀ Skip this stage
    Let  $\ell \leftarrow G_i(S).\ell$  and  $\Delta t_i \leftarrow t(S).t_i - t(S).t_{i-1}$ .
     $H \leftarrow (\Delta t_i)2^{-\ell}$ .
    If ( $H > \bar{h}$ )
       $S.\text{Bisect}(i)$ 
    Else
       $S.\text{EulerTube}(i)$ 
      Let  $G_i(S)$  be  $(\pi, g, \bar{\mu}^1, \bar{\mu}^2, \delta, \bar{h}, (\ell, E, F))$  after the Euler Tube.
      ▶ We must update  $\delta$  and  $\bar{h}$  for the next Euler Tube event.
       $G_i(S).\delta \leftarrow \delta/2$  ◀ (Updating the  $\delta$  target is easy)
      ▶ Updating  $\bar{h}$  to reflect the  $\delta$  requires six preparatory steps: (1)–(6)
      (1)  $E_i(S) \leftarrow E[2^\ell]$  ◀ End-enclosure for stage
      (2)  $F_i(S) \leftarrow \bigcup_{j=1}^{2^\ell} F[j]$  ◀ Full-enclosure for stage
      (3)  $\mu_2^i \leftarrow \max\{\bar{\mu}^2[j] : j = 1, \dots, 2^\ell\}$ 
      (4)  $\delta_1^i \leftarrow \text{TransformBound}(\delta, \pi, F_i(S))$ 
      (5)  $\bar{M} \leftarrow \|g^{[2]}(\pi(F_i(S)))\|_2$ 
      (6)  $htmp \leftarrow \min\{\Delta t_i, h_{\text{euler}}(\bar{h}, \bar{M}, \mu_2^i, \delta_1^i)\}$ 
       $G_i(S).\bar{h} \leftarrow htmp$  ◀ Finally, update  $\bar{h}$ 
    ◀ End of For-Loop
  ▶ The original code, " $E_0(S) \leftarrow \frac{1}{2}E_0(S)$ ," is replaced by the next lines:
  If  $e^{\bar{\mu}}(t_m(S) - t_0(S)) w_{\max}(E_0(S)) > \varepsilon_0/2$  ◀ CONDITION 1 (18) holds
     $E_0(S) \leftarrow \mathbf{p}_0 + \frac{1}{2}(E_0(S) - \mathbf{p}_0)$ 
   $r_0 \leftarrow w_{\max}(E_m(S))$ 
◀ End of While-Loop
Return  $S$ 

```

The optional argument \mathbf{p}_0 in (3) is passed to the enhance Refine. In the Refine of [23], $E_0(S)$ is updated by the simple line

$$E_0(S) \leftarrow \frac{1}{2}E_0(S) \quad (14)$$

to halve $E_0(S)$ at the end of the while-loop. We now shrink $E_0(S)$ conditionally, as indicated by the line in green. Moreover, we shrink $E_0(S)$ toward the point \mathbf{p}_0 ; the shrinkage step (14) is now

$$E_0(S) \leftarrow \mathbf{p}_0 + \frac{1}{2}(E_0 - \mathbf{p}_0). \quad (15)$$

Note that " $E_0 - \mathbf{p}_0$ " shifts E_0 so that \mathbf{p}_0 is at origin; after halving $\frac{1}{2}(E_0 - \mathbf{p}_0)$, we translate the origin of $\frac{1}{2}(E_0 - \mathbf{p}_0)$ back to \mathbf{p}_0 .

The enhancement amounts to trying to avoid unnecessary shrinkage of the initial enclosure E_0 . This is estimated as follows: recall that a **chain** is a sequence $C = (1 \leq k(1) \leq k(2) \leq \dots \leq k(m))$, such that EulerTube is invoked at phase-stage $(k(i), i)$ for each i . It is shown in [23, Appendix A, (H5)] that

$$r_m(C) \leq e^{\bar{\mu}}(r_0(C) + \Delta(C) m) = \underbrace{e^{\bar{\mu}}r_0(C)}_{r_0\text{-part}} + \underbrace{e^{\bar{\mu}}\Delta(C) m}_{\Delta\text{-part}}, \quad (16)$$

where $r_m(C)$ and $r_0(C)$ are one half of the maximal widths of the last and first end enclosures at the corresponding phases, respectively; $\bar{\mu}$ is the maximal logarithmic norm bound from the first phase; and $\Delta(C) = \max_{i=1}^m \delta(G_i(S))$ is evaluated at the initial phase of C . For a given chain C , if $2r_m(C) < \varepsilon_0$ then the Refine procedure halts. Hence, by (16), Refine will terminate as soon as both the r_0 -part and the Δ -part are bounded by $\varepsilon_0/4$; i.e., when

$$e^{\bar{\mu}}r_0(C) < \frac{\varepsilon_0}{4} \quad \text{and} \quad e^{\bar{\mu}}\Delta(C) m < \frac{\varepsilon_0}{4}. \quad (17)$$

To implement this logic in the Enhanced Refine, we specify three conditions:

$$\text{(CONDITION 1)} \quad \left(\frac{1}{2}w_{\max}(E_0(S))e^{\bar{\mu}} < \varepsilon_0/4\right) \quad (18)$$

$$\text{(CONDITION 2)} \quad \left(e^{\bar{\mu}}\delta(G_i(S))m < \varepsilon_0/8\right) \quad (19)$$

$$\text{(CONDITION 3)} \quad \left(e^{\bar{\mu}}\Delta m < \varepsilon_0/8\right) \text{ and } \left(\frac{1}{2}w_{\max}(E_0(S))e^{\bar{\mu}} < \varepsilon_0/4\right) \quad (20)$$

where $\Delta := \max_{i=1}^m \delta(G_i(S))$

In the Refine code, we test for these conditions and take corresponding actions:

- If CONDITION 1 holds, we do not shrink $E_0(S)$.
- If CONDITION 2 holds, we skip skip stage i .
- If CONDITION 3 holds, for all $i = 1, \dots, m$, we double value of $\delta(G_i(S))$ and invoke EulerTube, and exit Refine.

Note that (19) in CONDITION 2 requires $< \varepsilon_0/8$, rather than $< \varepsilon_0/4$ as in (17). This is because in S.Refine we always call EulerTube first and then halve δ . Consequently, when CONDITION 2 is detected to hold, the corresponding stage has just used twice the current value of δ and invoked EulerTube.

2.4 The End Cover Algorithm

We construct an ε -cover of $\text{End}_f(B_0, H)$ by invoking EndEnc, which returns a sequence of box pairs $\{(B_i, \bar{B}_i)\}_{i=1}^N$.

For the given initial box B_0 , if $B_0 \subseteq \bigcup_{i=1}^m \bar{B}_i$, then the union of the \bar{B}_i , namely $S := \bigcup_{i=1}^m \bar{B}_i$, constitutes a valid enclosure; in other words, $\text{EndCover}_f(B_0, \varepsilon, H) \rightarrow S$.

```

EndCoverf( $B_0, \varepsilon, H$ )  $\rightarrow S$ 
-----
INPUT:  $B_0 \subseteq \mathbb{R}^n, \varepsilon > 0, H > 0$ .
OUTPUT:  $S \subseteq \mathbb{R}^n$  satisfying
         $\text{End}_f(B_0, h) \subseteq S \subseteq (\text{End}_f(B_0, h) \oplus [\pm\varepsilon]^n)$ .

 $S_0 \leftarrow \{B_0\}, S \leftarrow \emptyset, P \leftarrow \emptyset$ 
While  $S_0 \neq \emptyset$ 
  Let  $B.\text{pop}(S_0) = \prod_{i=1}^n [a_i, b_i]$ 
   $\mathbf{p} = \text{mid}(B)$  ◀ Midpoint of  $B$ 
   $(B, \bar{B}) \leftarrow \text{EndEnc1}(B, \varepsilon, \mathbf{p}, H)$ 
  If ( $\bar{B} \neq B$ )
     $I_i^{k_i} := [a_i + \frac{k_i}{2}(b_i - a_i), a_i + \frac{k_i+1}{2}(b_i - a_i)]$ 
     $S_0 \leftarrow S_0 \cup \{\prod_{i=1}^n I_i^{k_i} : k_i \in \{0, 1\}\}$ .
   $S \leftarrow S \cup \bar{B}$ .
Return  $S$ .

```

3 Boundary Cover Problem

We now consider another approach to the End Cover Problem, by reducing it to a lower dimensional problem called **Boundary Cover Problem**. To provide the theoretical justification, we must introduce the concept of a "trajectory bundle".

3.1 Trajectory Bundles

We now use a more geometric language and call each $x \in \text{IVP}_f(\mathbf{p}_0, h)$ a trajectory. For any point \mathbf{p}_0 , the classic Picard-Lindelöf Theorem [7, 9] guarantees unique-existence of a single trajectory in $\text{IVP}_f(\mathbf{p}_0, h)$, for $h > 0$ small enough. For our validated algorithms, we must generalize point trajectories to "trajectory bundles".

A **trajectory** with **time-span** $[0, h]$ is a C^1 -function of the form $\phi : [0, h] \rightarrow \mathbb{R}^n$. Moreover, ϕ is a **f-trajectory** if $\phi \in \text{IVP}(B, h)$ for some $B \subseteq \mathbb{R}^n$ (i.e., $\phi'(t) = f(\phi(t))$ and $\phi(0) \in B$). Call

$$\Phi : [0, h] \times B \rightarrow \mathbb{R}^n \quad (21)$$

a **trajectory bundle** if $\Phi(\tau, \mathbf{p})$ is a continuous function on $[0, h] \times B$ such that $\Phi(0, \mathbf{p}) = \mathbf{p}$ (for all $\mathbf{p} \in B$) and satisfies the following **stratification property**:

$$\left(\forall \mathbf{p} \neq \mathbf{q} \in B \right) \left(\forall \tau \in [0, h] \right) \left[\Phi(\tau, \mathbf{p}) \neq \Phi(\tau, \mathbf{q}) \right]. \quad (22)$$

For all $\tau \in [0, h]$, $\mathbf{p} \in B$, we have the induced functions $\Phi|_{\mathbf{p}}$ and $\Phi|^\tau$

$$\left. \begin{array}{l} \Phi|_{\mathbf{p}} : [0, h] \rightarrow \mathbb{R}^n \quad (\mathbf{p}\text{-trajectory}), \\ \Phi|^\tau : B \rightarrow \mathbb{R}^n \quad (\tau\text{-end map}). \end{array} \right\} \quad (23)$$

where $\Phi|_{\mathbf{p}}(\tau) = \Phi|^\tau(\mathbf{p}) = \Phi(\tau, \mathbf{p})$. Call Φ a **f-bundle** on (B, h) . If each $\Phi|_{\mathbf{p}}$ is a **f-trajectory** ($\mathbf{p} \in B$), then denote this bundle by $\Phi = \Phi_{f,B,h}$. The stratification property (22) says that the graphs of the trajectories $\Phi|_{\mathbf{p}}$ and $\Phi|_{\mathbf{q}}$ for $\mathbf{p} \neq \mathbf{q}$ are pairwise disjoint. Before stating our bundle theorem, we need a useful lemma. Define $\text{Valid}_f(H)$ to be the set of all points $\mathbf{p} \in \mathbb{R}^n$ such that $\text{IVP}_f(\mathbf{p}, H)$ is valid.

LEMMA 1. *The set $\text{Valid}_f(H)$ is an open set for any $H > 0$.*

This lemma is trivial when $\text{Valid}_f(H)$ is empty since empty sets are open. Here is the bundle version the classic Picard-Lindelöf Theorem.

THEOREM 2 (GLOBAL PICARD-LINDELÖF BUNDLE).

If $f : \mathbb{R}^n \rightarrow \mathbb{R}^n$ is locally Lipschitz, and $B \subseteq \text{Valid}_f(H)$, then the f-bundle $\Phi_f(B, H)$ exists.

The bundle in this theorem is “global” because $H > 0$ is specified in advance. In contrast, the standard Picard-Lindelöf theorem only gives unique-existence of a “local” trajectory, i.e., for sufficiently small $h > 0$.

The End Map: If Φ is the trajectory bundle in (21), the τ -**slice** (for $\tau \in [0, h]$) of Φ is the set

$$\Phi|^\tau := \{\Phi(\tau, \mathbf{p}) : \mathbf{p} \in B\}. \quad (24)$$

E.g., the 0-slice is just B . The h -slice $\Phi|^\tau$ is called the **end-slice**. Define the **end map** of Φ to be

$$\text{End}_\Phi : B \rightarrow \mathbb{R}^n \quad (25)$$

where $\text{End}_\Phi(\mathbf{p}) = \Phi(h, \mathbf{p})$.

THEOREM 3. *Let $\Phi : [0, h] \times B \rightarrow \mathbb{R}^n$ be a trajectory bundle where $B \in \square \mathbb{R}^n$. Then the end map End_Φ of (25) is a homeomorphism from B onto the end-slice $\Phi|^\tau$.*

Note that our theorem holds even when $\dim(B) < n$; we need this generality in our boundary technique below. The proof of this theorem depends on a famous result of L.E.J. Brouwer (1912):

PROPOSITION 4. *Brouwer’s Invariance of Domain*

If U is an open set in \mathbb{R}^n and $f : U \rightarrow \mathbb{R}^n$ is continuous and injective, then $f(U)$ is also open. In particular, U and $f(U)$ are homeomorphic.

3.2 Reduction of End Cover to Boundary Cover

Theorem 3 justifies the following **Boundary Algorithm** for computing an ε -box cover of $\text{End}_f(B, h)$: if $B \in \square \mathbb{R}^n$, we compute an ε -box cover C_i ($i = 1, \dots, 2n$) for each of the $2n$ faces of B . Then

$$\bar{C} := \bigcup_{i=1}^{2n} C_i$$

is an ε -box cover for the boundary $\partial(\text{End}_f(B, h))$. Next, we compute a **filler cover** C_0 to cover the “interior” of $\bigcup \bar{C}$ so that $\bar{C} \cup C_0$ forms an ε -box cover of $\text{End}_f(B, h)$.

Thus, the Boundary Algorithm reduces an n -dimensional cover problem to several $(n-1)$ -dimensional ones, modulo the **Fill Problem** of computing C_0 ; the header for this problem is thus

$$\text{Filler}(\bar{C}, \varepsilon) \rightarrow C_0$$

Unfortunately, this appears to be an ill-formed problem unless ε is small enough.

To understand the difficulty, note that $\bigcup \bar{C}$ is a connected set. The boundary of $\bigcup \bar{C}$ is the union of finitely many components, $S_0 \cup S_1 \cup \dots \cup S_k$ where each S_j is topologically an $(n-1)$ -sphere. Moreover, S_0 is the unique exterior component such that the other S_i 's ($i = 1, \dots, k$) lies in the interior of S_0 . Also the S_i 's are not nested (if S_i is contained in some S_j then $j = 0$). We want the filler set C_0 to lie inside S_0 , and to cover up *some* of these S_i 's. But identifying the S_i 's to cover is a non-trivial problem especially in higher dimensions. Let us say that ε is **small enough** if $k = 1$. If ε is small enough, then the boundary $\partial(\bigcup \bar{C})$ has two components S_0, S_1

with S_1 inside S_0 . The boxes of C_0 just have to cover the interior of S_1 but stay within S_0 . This is a relatively simpler problem of computational geometry, with no need for any IVP solving. In our examples ($n = 2$), we can visually see that our ε is small enough. In our experimental section, we will compare this Boundary Algorithm with $\text{EndCover}_f(B_0, \varepsilon)$.

4 Complexity Analysis

This section provides a complexity analysis of our EndCover algorithm in Subsection 2.4. Two preliminary remarks are necessary: (C1) One might expect the complexity of EndCover to be a function of the input instance (E_0, ε, H) , and also f . But we do this indirectly, via two derived⁵ parameters \bar{h} and \bar{B} defined as follows:

$$\bar{B} = \bar{B}(E_0, H, \varepsilon) := \sum_{i=0}^{k-1} [0, H]^i f^{[i]}(E_0) + \text{Box}(\varepsilon), \quad (26)$$

$$\bar{h} = \bar{h}(E_0, H, \varepsilon) := \min \left\{ H, \min_{i=1}^n \left(\frac{\varepsilon_i}{M_i} \right)^{1/k} \right\}, \quad (27)$$

where

$$M_i := \sup_{\mathbf{p} \in \bar{B}(E_0, H, \varepsilon)} \left| (f^{[k]}(\mathbf{p}))_i \right|, \quad (i = 1, \dots, n) \quad (28)$$

(C2) Second, our complexity counts the number of **steps**, defined to be either assignments (e.g., $x \leftarrow F(y)$) or if-tests (e.g., “If $(H > \hat{h})$ ”) in our pseudo-codes for Extend , Refine , EulerTube , Bisect , etc. The **non-steps** in pseudo-codes are the subroutine calls as well as while- and for-statements. The overall number of steps can be bounded if we bound the number of iterations in while- and for-loops. Each step takes $O(1)$ time for fixed f, E_0, ε, H . But some assignments appear violate this. E.g. lines (2) and (3) in Refine appear to take $\Omega(2^l)$ steps. But it is not hard to re-factor our code so that they are truly $O(1)$.

⁵See [23, Lemma 7]. To be consistent with Lemma 7, we use the more general error bound $\varepsilon = (\varepsilon_1, \dots, \varepsilon_n)$ instead of $\varepsilon > 0$.

In principle, our step complexity could be translated into the standard bit-complexity model based on Turing machines, more or less routinely.

4.1 Complexity of End Enclosure

We first analyze the complexity of the EndEnclosure Algorithm, since it is called by the EndCover Algorithm. There are 3 components:

- (1) The total number of calls to Extend and Refine, i.e., the number of stages generated by the EndEnc1 algorithm;
- (2) The complexity of a single call to Extend;
- (3) The complexity of a single call to Refine.

4.1.1 Bound on the number of stages. We first bound the number of stages produced by the EndEnc algorithm:

LEMMA 5.

The number of stages in EndEnc1($E_0, \epsilon; \mathbf{p}, H$) is at most $1 + \lceil H/\bar{h} \rceil$ where $\bar{h} = \bar{h}(\bar{E}, H, \epsilon)$, see (27) and $\bar{E} = \text{Image}_f(E_0, H) + \text{Box}(\epsilon)$.

4.1.2 Complexity of Extend. The subroutine $\mathcal{S}.\text{Extend}$ appends a new stage to scaffold \mathcal{S} . This is accomplished by one call each of StepA and StepB, together with some auxiliary operations, in order to construct admissible triples and validated enclosures. All these are loop-free operations except for StepA. E.g., StepB basically performs Taylor expansions of order k for an n -dimensional system, and counts as $O(1)$ steps.

LEMMA 6 (EXTEND). Given a scaffold \mathcal{S} with m stages and parameters $\epsilon > 0$ and $H > 0$, the subroutine StepA executed within $\mathcal{S}.\text{Extend}(\epsilon, H)$ performs at most

$$\left\lceil \log_2 \left(\frac{H}{\bar{h}} \right) \right\rceil$$

iterations, where $\bar{h} = \bar{h}(E_m(\mathcal{S}), H, \epsilon)$ is defined in (27)

4.1.3 Complexity of Refine. The complexity of Refine is $O(1 + N_0)$ where N_0 is the maximum of N_1 and N_2 where N_1 is the number of phases needed to satisfy condition (18), and N_2 is the number of phases needed to satisfy condition (19) for every stage. After N_0 phases, we need one more phase in which every stage will call EulerTube to form a chain. By (16), Refine terminates. The “1+” refers to this last phase.

LEMMA 7 (REFINE). Let \mathcal{S} be an m -stage scaffold, and $\epsilon_0 > 0$. For each stage i write $\Delta t_i = t_{i+1}(\mathcal{S}) - t_i(\mathcal{S})$ and

$$G_i(\mathcal{S}) = ((\pi_i, \mathbf{g}_i), (\ell_i, \mathbf{E}_i, \mathbf{F}_i), (\bar{\boldsymbol{\mu}}_i^1, \bar{\boldsymbol{\mu}}_i^2), (\delta_i, \hat{h}_i)).$$

The number of phases in $\mathcal{S}.\text{Refine}(\epsilon_0)$ is at most $1 + N_0$ where

- $N_0 := \max \{N_1, N_2\}$,
- $N_1 := \left\lceil \log_2 \frac{2 w_{\max}(E_0(\mathcal{S})) e^{\bar{\mu}}}{\epsilon_0} \right\rceil$,
- $N_2 := \#\text{EulerTube} + \#\text{Bisection}$
- $\#\text{EulerTube} := \left\lceil \log_2 \frac{8m \Delta_{\max} e^{\bar{\mu}}}{\epsilon_0} \right\rceil$
- $\#\text{Bisection} := \left\lceil \max_{i=1, \dots, m, p \in I_i} \left(\log_2 \left(\frac{\Delta t_i}{h^{\text{euler}}(\Delta t_i, M_i, p, \delta'_i)} \right) \right) \right\rceil$
- Moreover, $I_i = \left[\min_{\mathbf{q} \in \pi(F_i(\mathcal{S}))} (\mu_2(J_{\mathbf{g}_i}(\mathbf{q}))), \max_{i=1, \dots, m} (\max \bar{\boldsymbol{\mu}}_i^2) \right]$,

- $\bar{\mu} := \max_{i=1, \dots, m} (\max \bar{\boldsymbol{\mu}}_i^1)$, $\Delta_{\max} := \max_{i=1, \dots, m} \delta_i$,
- $M_i := \|\mathbf{g}_i^{[2]}(\pi(F_i(\mathcal{S}))\|_2$,
- $\delta'_i := \text{TransformBound} \left(\min \left(\delta_i, \frac{\epsilon_0}{16me^{\bar{\mu}}} \right), \pi, F_i(\mathcal{S}) \right)$.

4.1.4 Complexity of EndEnc1. By Lemma 5, EndEnc1 will generate $\leq 1 + \lceil H/\bar{h} \rceil$ stages. Within each stage, the Extend and Refine subroutines are called once, and their complexity are bounded as in Lemma 6 and Lemma 7. It follows that the step complexity of EndEnc1 is

$$O \left((H/\bar{h}) \cdot ((\log_2(H/\bar{h}) + N_0)) \right) \quad (29)$$

4.2 Complexity of EndCover

We return from the analysis of EndEnc1 to our EndCover algorithm. This higher-level procedure orchestrates multiple calls to EndEnc1, and understanding its complexity requires integrating the insights from the subroutine analyses.

To complete the picture, we now bound the number of times EndCover invokes EndEnc1. The following theorem addresses this:

THEOREM 8. Let $\bar{B} = \text{image}(\text{IVP}(B_0, H)) + \text{Box}(\epsilon)$ and $\bar{\mu} = \mu_2(J_f(\bar{B}))$. Then EndCover(B_0, H, ϵ) will call EndEnc1 at most

$$\Theta \left(\left(\frac{2w_{\max}(B_0)e^{\bar{\mu}}}{\epsilon} \right)^n \right)$$

times.

5 Experiments

This section presents empirical evaluations to demonstrate the practical efficacy and advantages of our proposed algorithms. Our experiments are based on the ODE models given in Table 1. Our open source C++ programs (include an executable), data, Makefile are available in our project home [3]. All timings are taken on a laptop with a 13th Gen Intel Core i7-13700HX 2.10 GHz processor and 16.0 GB RAM.

LIMITATION: Our current implementation are based machine-precision arithmetics. As explained in Subsection 1.2, in principle, we could achieve rigorous arbitrary precision implementation. This is future plan.

5.1 Comparison with other validated Solvers

Table 2 contains the performances of four validated interval IVP solvers on the models in Table 1. These solvers are:

- (1) “Ours” refers to the EndCover_Algo in this paper.
- (2) StepB_{Direct} (see [23]), viewed as a “baseline algorithm” since it uses the standard iterative scheme that alternates between stepA and stepB, with stepB using the direct method.
- (3) “VNODE-LP” from Nedialkov [13, 19]. It implements Lohner’s method.
- (4) “CAPD” [20] that implements Cr-Lohner method (using $r = 3$ in their software).

Each solver is tasked with computing the end-enclosure for IVP(B_0, T) under identical conditions. Since “Ours” outputs a set of boxes, we take the smallest bounding box of their union. Thus, the reported enclosure is a over-approximation of our true output.

Efficacy of our method. Define the **efficacy ratio** of some method “Other” relative to “Ours” as $\rho(\text{Others}) := \frac{w_{\max}(\text{Others})}{w_{\max}(\text{Ours})}$. So

Eg*	Name	$f(x)$	Parameters	Box B_0	Reference
Eg1	Lotka-Volterra Predator-Prey	$(ax(1-y), -by(1-x))$	$(a, b) = (2, 1)$	$\text{Box}_{(1,3)}(0,1)$	[11], [2, p.13]
Eg2	Van der Pol	$(y, -c(1-x^2)y - x)$	$c = 1$	$\text{Box}_{(-3,3)}(0,1)$	[2, p.2]
Eg3	Asymptote	$(x^2, -y^2 + 7x)$	N/A	$\text{Box}_{(-1.5,8.5)}(0,0.1)$	N/A
Eg4	Quadratic	(y, x^2)	N/A	$\text{Box}_{(1,-1)}(0,0.5)$	[2, p.11]
Eg5	FitzHugh-Nagumo	$(x - \frac{x^3}{3} - y + I, \epsilon(x + a - by))$	$(a, b, \epsilon, I) = (0.7, 0.8, 0.08, 0.5)$	$\text{Box}_{(1,0)}(0,1)$	[17]
Eg6	Reduced Robertson (2D)	$(-k_1 x + k_2 y(1-x-y), k_1 x - k_2 y(1-x-y) - k_3 y^2)$	$(k_1, k_2, k_3) = (0.04, 10^4, 3 \times 10^7)$	$\text{Box}_{(1,0)}(10^{-6})$	[8]
Eg7	Lorenz	$(\sigma(y-x), x(\rho-z) - y, xy - \beta z)$	$(\sigma, \rho, \beta) = (10, 28, 8/3)$	$\text{Box}_{(15,15,36)}(0,0.01)$	[2, p.11]
Eg8	Rössler	$(-y - z, x + ay, b + z(x - c))$	$(a, b, c) = (0.2, 0.2, 5.7)$	$\text{Box}_{(1,2,3)}(0,1)$	[14]

Table 1: List of IVP Problems

$\rho(\text{Other}) > 1$ means “Ours” is more efficacious. The efficacy column in Table 2 demonstrates that $\rho(\text{Other}) > 1$ for all but one entry (0.95 in blue). Note that $\rho(\text{Other})$ increases as T increases.

Robustness of our method. Table 2 shows 3 kinds of abnormal behavior: **Timeout** (if it takes longer than 30 minutes), **No Output** (the code stops without output, or returns error), and **Invalid**. The **No Output** behavior is seen with CAPD: see Eg1 with $T = 5.5$, Eg2 with $T = 2$, Eg5 with $T = 4$, and Eg7 with $T = 4$. The **Invalid** behavior is seen in VNODE-LP, meaning that its step size has gone below some threshold: see Eg1 with $T = 5.5$, Eg2 with $T = 2$, and Eg7 with $T = 4$. However, “Ours” do not show any of these abnormal behavior, i.e., it is robust.

5.2 Comparing EndCover with BoundaryCover

The standard iterative IVP algorithms (e.g., StepB_{Direct}) suffers from the wrapping effect, and must use Lohner’s matrix transformation. However, our EndCover and BoundaryCover reduces the wrapping effect by tracking the boundary with smaller boxes. This leads to improved numerical stability. Furthermore, our Refine algorithm prevents the intermediate enclosures from becoming excessively large; thus we avoid unnecessary step-size reductions leading to loss of precision. When T is small, the BoundaryCover method is slower than the EndCover method. But when T is large, the Boundary method becomes faster since it only needs to handle the boundary; see Eg1, Eg2, Eg4, Eg5 in Table 2.

6 Conclusion

We have designed a complete validated algorithm for the reachability form of the IVP problem, called the End Cover Problem. We also offer an alternative technique based on covering the boundary of the End Cover as a lower-dimensional problem (and thus possibly faster). Preliminary implementations show that our algorithms are practical, robust, and outperforms state-of-the-art validated algorithms (CAPD and VNODE-LP).

References

- [1] A. G. Bachrach. *Trajectory bundle estimation For perception-driven planning*. Ph.D. thesis, M.I.T., 2013.
- [2] F. Bünger. A Taylor Model Toolbox for solving ODEs implemented in MATLAB/INTLAB. *J. Comp. and Appl. Math.*, 368:112511, 2020.
- [3] Core Library Homepage, since 1999. Software download, source, documentation and links: https://cs.nyu.edu/exact/core_pages/svn-core.html. You can navigate to the ivp project, or go directly to <https://subversive.cims.nyu.edu/exact/corelib2/trunk/progs/ivp>.
- [4] G. F. Corliss. Survey of interval algorithms for ordinary differential equations. *Appl. Math. Comp.*, 31, 1989.
- [5] C. Fan, K. Miller, and S. Mitra. Fast and guaranteed safe controller synthesis for nonlinear vehicle models. In S. K. Lahiri and C. Wang, editors, *Computer Aided Verification*, pages 629–652, Cham, 2020. Springer International.
- [6] O. Goldreich. On Promise Problems (a survey). In *Theoretical Computer Science: Essays in memory of Shimon Even*, pages 254 – 290. Springer, 2006. LNCS. Vol. 3895.
- [7] E. Hairer, S. P. Nørsett, and G. Wanner. *Solving Ordinary Differential Equations I: Nonstiff Problems*. Springer-Verlag, Berlin, second revised edition, 2008.
- [8] E. Hairer and G. Wanner. *Solving Ordinary Differential Equations II: Stiff and Differential-Algebraic Problems*. Springer-Verlag, Berlin, second revised, corrected edition, 2002.
- [9] J. H. Hubbard and B. H. West. *Differential Equations, A Dynamical Systems Approach. Part I: Ordinary Differential Equations*. Springer-Verlag, 1991. The 3d Edition (1997) dropped the Part I designation.
- [10] T. Kapela, M. Mrozek, D. Wilczak, and P. Zgliczyński. CAPD::DynSys: a flexible C++ toolbox for rigorous numerical analysis of dynamical systems. *Communications in Nonlinear Sci. and Numerical Simulation*, 101:105578, 2021.
- [11] R. Moore. Interval Analysis: Differential Equations. In C. A. Floudas and P. M. Pardalos, editors, *Encyclopedia of Optimization*, pages 1686–1689. Springer, 2nd edition, 2009.
- [12] R. E. Moore. *Interval Analysis*. Prentice Hall, Englewood Cliffs, NJ, 1966.
- [13] N. S. Nedialkov, K. R. Jackson, and G. F. Corliss. Validated solutions of initial value problems for ordinary differential equations. *Applied Mathematics and Computation*, 105(1):21–68, 1999.
- [14] O. Rössler. An equation for continuous chaos. *Physics Letters A*, 57(5):397–398, 1976.
- [15] W. Rudin. *Principles of Mathematical Analysis*. McGraw-Hill, New York, 3rd edition, 1976.
- [16] K. Shen, D. L. Robertson, and J. K. Scott. Tight reachability bounds for constrained nonlinear systems using mean value differential inequalities. *Automatica*, 134:109911, 2021.
- [17] W. E. Sherwood. *FitzHugh–Nagumo Model*, pages 1–11. Springer New York, 2013.
- [18] K. Tracy, J. Zhang, J. Arrizabalaga, S. Schaal, Y. Tassa, T. Erez, and Z. Manchester. The trajectory bundle method: Unifying sequential-convex programming and sampling-based trajectory optimization, Sept. 2025.
- [19] VNODE-LP Homepage, Access 2026. Software download, source, documentation and links: <https://www.cas.mcmaster.ca/nedialk/vnodelp>.
- [20] D. Wilczak and P. Zgliczyński. C^r -Lohner algorithm. *Schedae Informaticae*, 20:9–42, 2011.
- [21] J. Xu and C. Yap. Effective subdivision algorithm for isolating zeros of real systems of equations, with complexity analysis. In *Int’l Symp. Symbolic and Alge. Comp. (44th ISSAC)*, pages 355–362, New York, 2019. ACM Press. July 15-18. Beijing.
- [22] C. K. Yap and V. Sharma. Robust geometric computation. In M.-Y. Kao, editor, *Encyclopedia of Algorithms*, pages 788–790. Springer, 2008.
- [23] B. Zhang and C. Yap. A Novel Approach to the Initial Value Problem with a Complete Validated Algorithm. *arXiv preprint arXiv:2502.00503*, Feb. 2025.
- [24] B. Zhang and C. Yap. End cover for initial value problem: Complete validated algorithms with complexity analysis. *arXiv preprint arXiv:2602.00162*, Feb. 2026.

Case	Method	T	$B_1 = (\text{mid}) \pm (\text{rad})$	$\frac{w_{\max}(\text{others})}{w_{\max}(\text{ours})}$	Time (s)	
Eg1	Ours	2.00	$(0.08, 0.57) \pm (0.02, 0.02)$	1	0.02 0.05	
	StepB _{Direct}		$(0.08, 0.58) \pm (0.16, 0.13)$	6.66	0.52	
	VNODE-LP		$(0.08, 0.58) \pm (0.04, 0.05)$	2.26	0.17	
	CAPD		$(0.08, 0.58) \pm (0.05, 0.05)$	2.12	0.01	
	Ours	4.00	$(1.46, 0.19) \pm (0.40, 0.05)$	1	0.13 0.08	
	StepB _{Direct}		Timeout	N/A	Timeout	
	VNODE-LP		$(1.43, 0.34) \pm (3.23, 0.91)$	8.07	0.39	
	CAPD		$(1.45, 0.19) \pm (3.38, 0.88)$	8.35	0.02	
	Ours	5.50	$(1.14, 2.95) \pm (0.67, 0.49)$	1	3.42 1.21	
	StepB _{Direct}		Timeout	N/A	Timeout	
	VNODE-LP		Invalid	N/A	Invalid	
	CAPD		No Output	N/A	No Output	
Eg2	Ours	1.00	$(-2.13, 0.57) \pm (0.25, 0.21)$	1	0.02 0.04	
	StepB _{Direct}		$(-2.13, 0.57) \pm (0.26, 0.23)$	1.03	0.51	
	VNODE-LP		$(-2.15, 0.58) \pm (0.90, 3.49)$	13.95	0.17	
	CAPD		$(-2.13, 0.56) \pm (0.29, 0.28)$	1.15	0.02	
	Ours	2.00	$(-1.41, 0.96) \pm (0.38, 0.35)$	1	0.77 0.14	
	StepB _{Direct}		Timeout	N/A	Timeout	
Eg3	StepB _{Direct}	1.00	Invalid	N/A	Invalid	
	VNODE-LP		No Output	N/A	No Output	
	CAPD					
	Ours		$(-0.60, -6.69) \pm (0.00, 0.18)$	1	0.02 0.07	
Eg4	StepB _{Direct}	1.00	$(-0.60, -6.69) \pm (0.01, 0.19)$	1.01	4.11	
	VNODE-LP		$(-0.60, -6.69) \pm (0.00, 0.19)$	1.05	0.20	
	CAPD		$(-0.60, -6.69) \pm (0.01, 0.19)$	1.01	0.02	
	Ours		$(0.28, -0.58) \pm (0.15, 0.16)$	1	0.01 0.02	
	StepB _{Direct}	4.00	$(0.28, -0.59) \pm (0.16, 0.17)$	1.06	0.01	
	VNODE-LP		$(0.28, -0.59) \pm (0.16, 0.18)$	1.10	0.03	
	CAPD		$(0.28, -0.59) \pm (0.16, 0.17)$	1.06	0.01	
	Ours		$(-0.65, 0.25) \pm (0.24, 0.57)$	1	0.12 0.06	
Eg5	StepB _{Direct}	1.00	$(-0.68, 0.34) \pm (1.01, 2.12)$	3.71	0.01	
	VNODE-LP		$(0.59, 2.53) \pm (22.57, 88.77)$	155.74	0.09	
	CAPD		$(-0.68, 0.34) \pm (7.51, 25.53)$	44.79	0.01	
	Ours		$(1.76, 0.17) \pm (0.11, 0.10)$	1	0.03 0.07	
	StepB _{Direct}	4.00	$(1.76, 0.17) \pm (0.17, 0.10)$	1.55	0.01	
	VNODE-LP		$(1.76, 0.17) \pm (0.10, 0.10)$	0.95	0.09	
	CAPD		$(1.76, 0.17) \pm (0.18, 0.10)$	1.66	0.02	
	Ours		$(1.68, 0.68) \pm (0.08, 0.10)$	1	1.22 0.13	
	Eg6	StepB _{Direct}	1.00	Timeout	N/A	Timeout
		VNODE-LP		$(1.68, 0.68) \pm (0.07, 0.11)$	1.13	0.41
CAPD		No Output		N/A	No Output	
Ours		$(0.97, 0.00) \pm (0.00, 0.00)$		1	15.86 63.35	
StepB _{Direct}		1.00	Timeout	N/A	Timeout	
VNODE-LP			$(0.97, 0.00) \pm (0.00, 0.00)$	1.00	11.06	
Eg7	CAPD	1.00	$(0.97, 0.00) \pm (0.00, 0.00)$	1.00	16.39	
	Ours		$(-6.9, 3.0, 35.1) \pm (0.03, 0.01, 0.04)$	1	0.12 0.65	
	StepB _{Direct}		$(-6.9, 3.0, 35.1) \pm (37.40, 228.27, 225.31)$	5692.51	7.35	
	VNODE-LP		$(-6.95, 3.00, 35.14) \pm (0.03, 0.01, 0.04)$	1.03	0.66	
	CAPD	4.00	$(-6.95, 3.00, 35.14) \pm (0.03, 0.01, 0.04)$	1.02	0.10	
	Ours		$(-4.75, -0.01, 29.07) \pm (0.09, 0.09, 0.11)$	1	4.03 12.55	
	StepB _{Direct}		Timeout	N/A	Timeout	
	VNODE-LP		Invalid	N/A	Invalid	
	Eg8	CAPD	1.00	No Output	N/A	No Output
		Ours		$(-1.73, 1.87, 0.03) \pm (0.15, 0.17, 0.00)$	1	0.03 0.16
		StepB _{Direct}		$(-1.73, 1.87, 0.03) \pm (0.27, 0.29, 0.00)$	1.72	0.01
		VNODE-LP		$(-1.74, 1.86, 0.03) \pm (0.15, 0.18, 0.00)$	1.04	0.08
CAPD		4.00	$(-1.73, 1.87, 0.03) \pm (0.15, 0.17, 0.00)$	1.02	0.02	
Ours			$(1.95, -2.89, 0.05) \pm (0.20, 0.23, 0.00)$	1	0.08 0.45	
StepB _{Direct}			$(1.95, -2.89, 0.05) \pm (11.67, 8.86, 67.65)$	292.99	1.45	
VNODE-LP			$(1.96, -2.88, 0.05) \pm (0.21, 0.24, 0.00)$	1.04	0.28	
CAPD	4.00	$(1.95, -2.89, 0.05) \pm (0.21, 0.23, 0.00)$	1.02	0.07		

Table 2: Performance comparison of EndCover with existing methods under $\varepsilon = 1.0$. For our method, the reported time consists of two values separated by $a | b$, where a denotes the computation time using the End cover and b denotes the computation time using the Boundary cover. The reported B_1 for our method is obtained by taking the minimal enclosing box of the Boundary cover.

A Appendix: Proofs

The numberings of lemmas and theorems in this Appendix are the same as the corresponding results in the text; they are also hyperlinked to the text.

Theorem 3

Let $\Phi : [0, h] \times B \rightarrow \mathbb{R}^n$ be a trajectory bundle where $B \in \square\mathbb{R}^n$. Then the end map End_Φ of (25) is a homeomorphism from B onto the end-slice $\Phi|_h$.

Proof. The map (25) has two properties:

- (a) It is continuous (this follows from the continuity of Φ).
- (b) It is injective (this is the stratification property).

If U is the interior of B , then Brouwer's Invariance of Domain implies U is homeomorphic to $\text{End}_\Phi(U)$. But the closure of $\text{End}_\Phi(U)$ is the end-slice $\Phi|_h$. Part(b) above says that $\text{End}_\Phi : B \rightarrow \Phi|_h$ is injective. This implies that End_Φ is a homeomorphism ([15, Theorem 4.17, p.90]). **Q.E.D.**

Lemma 5

The number of stages in $\text{EndEnc1}(E_0, \epsilon; \mathbf{p}, H)$ is at most $1 + \lceil H/\bar{h} \rceil$ where $\bar{h} = \bar{h}(\bar{E}, H, \epsilon)$, see (27) and $\bar{E} = \text{image}(\text{IVP}(E_0, H)) + \text{Box}(\epsilon)$.

Proof. Since $\text{IVP}(B_0, H)$ is valid, \bar{E} is bounded. The set $\bar{B} = \bar{B}(\bar{E}, H, \epsilon)$ is also bounded as it is constructed from bounded sets using continuous operations. Since $f^{[k]}$ is continuous on the compact set \bar{B} , each \bar{M}_i ($i = 1, \dots, n$) in the definition (28) of $\bar{h} = \bar{h}(\bar{E}, H, \epsilon)$ is finite. Thus, $0 < \bar{h} \leq \min_{i=1}^n \left(\epsilon_i / \bar{M}_i \right)^{1/k}$. Suppose the algorithm terminates after m stages. Then the time sequence of the final scaffold has the form $\mathbf{t} = (t_0, t_1, \dots, t_m)$ where $(t_0, t_m) = (0, H)$. The $(j-1)$ th stage was extended to the j th stage by calling $\text{StepA}(E_{j-1}, H - t_{j-1}, \epsilon) \rightarrow (h_j, F_j)$. Clearly, $h_j = t_j - t_{j-1}$. By (27),

$$h_j \geq \min \left\{ H - t_{j-1}, \min_{i=1}^n \left(\frac{\epsilon_i}{\bar{M}_i} \right)^{1/k} \right\}.$$

If $h_j = H - t_{j-1}$, then j must be the final stage ($j = m$). Therefore, for every $j < m$, $h_j \geq \min_{i=1}^n \left(\frac{\epsilon_i}{\bar{M}_i} \right)^{1/k}$. We claim that for all $j = 1, \dots, m-1$, one has $h_j \geq \bar{h}$. This immediately yields $(m-1)\bar{h} \leq H$, hence $m \leq 1 + \lceil H/\bar{h} \rceil$. To prove the claim, fix any $j < m$. Then

$$\begin{aligned} h_j &\geq \min_{i=1}^n \left(\epsilon_i / M_i \right)^{1/k} && \text{(since } j < m) \\ &\geq \min_{i=1}^n \left(\epsilon_i / \bar{M}_i \right)^{1/k} && \text{(since } M_i \leq \bar{M}_i) \\ &\geq \bar{h} && \text{(by definition of } \bar{h}) \end{aligned}$$

The above inequality $M_i \leq \bar{M}_i$ comes from the inclusion

$$\bar{B}(E_{j-1}, H - t_{j-1}, \epsilon) \subseteq \bar{B}(\bar{E}, H, \epsilon),$$

and the definition of M_i, \bar{M}_i in terms of these two sets. This establishes $m - 1 \leq H/\bar{h}$ as required. **Q.E.D.**

Lemma 6 (EXTEND)

Given a scaffold \mathcal{S} with m stages and parameters $\epsilon > 0$ and $H > 0$, the subroutine StepA executed within $\mathcal{S}.\text{Extend}(\epsilon, H)$ performs at most

$$\left\lceil \log_2 \left(\frac{H}{\bar{h}} \right) \right\rceil$$

iterations, where $\bar{h} = \bar{h}(E_m(\mathcal{S}), H, \epsilon)$ is defined in (27)

Proof. The Extend subroutine will call StepA which performs a binary search by halving the step size H until an admissible pair $(h > H/2, F)$ is found. The number of halvings required is $O(\log_2(H/\bar{h}))$, as H is reduced to a minimum step size bounded below by $\bar{h} > 0$. **Q.E.D.**

Lemma 7 (REFINE)

Let \mathcal{S} be an m -stage scaffold, and $\epsilon_0 > 0$. For each stage i write $\Delta t_i = t_{i+1}(\mathcal{S}) - t_i(\mathcal{S})$ and

$$G_i(\mathcal{S}) = ((\pi_i, \mathbf{g}_i), (\ell_i, \mathbf{E}_i, F_i), (\bar{\mu}_i^1, \bar{\mu}_i^2), (\delta_i, \hat{h}_i)).$$

The number of phases in $\mathcal{S}.\text{Refine}(\epsilon_0)$ is at most $1 + N_0$ where

- $N_0 := \max \{N_1, N_2\}$,
- $N_1 := \left\lceil \log_2 \frac{2 w_{\max}(E_0(\mathcal{S})) e^{\bar{\mu}}}{\epsilon_0} \right\rceil$,
- $N_2 := \#\text{EulerTube} + \#\text{Bisection}$
- $\#\text{EulerTube} := \left\lceil \log_2 \frac{8m \Delta_{\max} e^{\bar{\mu}}}{\epsilon_0} \right\rceil$
- $\#\text{Bisection} := \left\lceil \max_{i=1, \dots, m, p \in I_i} \left(\log_2 \left(\frac{\Delta t_i}{h^{\text{euler}}(\Delta t_i, M_i, p, \delta_i')} \right) \right) \right\rceil$
- Moreover, $I_i = \left[\min_{\mathbf{q} \in \pi(F_i(\mathcal{S}))} (\mu_2(J_{\mathbf{g}_i}(\mathbf{q}))), \max_{i=1, \dots, m} (\max \bar{\mu}_i^2) \right]$,
- $\bar{\mu} := \max_{i=1, \dots, m} (\max \bar{\mu}_i^1)$,
- $\Delta_{\max} := \max_{i=1, \dots, m} \delta_i$,
- $M_i := \|\mathbf{g}_i^{[2]}(\pi(F_i(\mathcal{S})))\|_2$,
- $\delta_i' := \text{TransformBound} \left(\min \left(\delta_i, \frac{\epsilon_0}{16me^{\bar{\mu}}} \right), \pi, F_i(\mathcal{S}) \right)$.

Proof. N_1 is the number of phases needed to satisfy condition (18). Since in each phase we halve $w_{\max}(E_0(\mathcal{S}))$, after

$$N_1 := \left\lceil \log_2 \frac{2 w_{\max}(E_0(\mathcal{S})) e^{\bar{\mu}}}{\epsilon_0} \right\rceil$$

phases, condition (18) is satisfied.

Next, we consider the phases required for condition (19). Fix a stage i . Note that in each phase, the value δ_i is either halved or left unchanged; once δ_i satisfies (19) it is never modified again.

By condition (19), $\delta_i < \frac{\epsilon_0}{8me^{\bar{\mu}}}$ and $\delta_i \leq \Delta_{\max}$, so the number of phases in which δ_i is halved is at most

$$\#\text{EulerTube} := \left\lceil \log_2 \frac{8m \Delta_{\max} e^{\bar{\mu}}}{\epsilon_0} \right\rceil.$$

Now we count the phases where δ_i stays unchanged. During Refine, if δ_i is not changed in a phase, then Bisect is called in that phase. Hence it suffices to count the number of calls to Bisect. A call to Bisect occurs exactly when the current mini-step size, i.e., $\frac{\Delta t_i}{2^l}$, exceeds h^{euler} . Thus we need a lower bound for h^{euler} .

Recall that whenever the logarithmic norm μ is positive, we transform the system by π , which yields a new system with a negative logarithmic norm. Consequently (see [23, Eq. (12)])

$$h^{\text{euler}}(H, \bar{M}, \mu, \delta) = \min\left\{H, \frac{2\mu\delta}{M(e^{\mu H} - 1) - \mu^2\delta}\right\}.$$

$h^{\text{euler}}(H, \bar{M}, \mu, \delta)$ is decreasing in \bar{M} and increasing in δ . During refinement the set $F_i(S)$ shrinks, hence $M_i = \|\mathbf{g}_i^{[2]}(\pi(F_i(S)))\|_2$ provides an upper bound for the parameter \bar{M} in stage i . Moreover, condition (19) guarantees that $\min(\delta_i, \frac{\varepsilon_0}{16me^{\bar{\mu}}})$ is a lower bound for $\delta(G_i(S))$. Therefore δ'_i is a lower bound for the δ -parameter in stage i . Finally, by definition of I_i , the parameter μ in the i -th stage always lies in I_i .

Consequently, for stage i the Euler step size is bounded below by $\min_{p \in I_i} h^{\text{euler}}(\Delta t_i, M_i, p, \delta'_i)$. Hence the number of calls to Bisect

for the i -th stage is at most $\max_{p \in I_i} \log_2\left(\frac{\Delta t_i}{h^{\text{euler}}(\Delta t_i, M_i, p, \delta'_i)}\right)$.

Thus, N_2 is the number of phases needed to satisfy condition (19) for every stage. **Q.E.D.**

Theorem 8

Let $\bar{B} = \text{image}(\text{IVP}(B_0, H)) + \text{Box}(\varepsilon)$ and $\bar{\mu} = \mu_2(J(f(\bar{B})))$. Then $\text{EndCover}(B_0, H, \varepsilon)$ will call EndEnc1 at most

$$\Theta\left(\left(\frac{2w_{\max}(B_0)e^{\bar{\mu}H}}{\varepsilon}\right)^n\right)$$

times.

Proof. Each call of EndEnc1 returns two boxes \underline{B}_i and \bar{B}_i . We bound the number of indices i for which the collection $\{\underline{B}_i\}$ can cover B_0 .

From (18), every box \underline{B}_i satisfies a uniform positive bound on its size: $\frac{\varepsilon}{4e^{\bar{\mu}H}} < w_{\max}(\underline{B}) < \frac{\varepsilon}{2e^{\bar{\mu}H}}$. Consequently, starting from an initial box B , the number of subdivisions needed to obtain a box whose size is below this lower bound is at most $\left\lceil \log_2 \frac{4w_{\max}(B)e^{\bar{\mu}H}}{\varepsilon} \right\rceil$. Hence, along each coordinate direction, the number of such subdivisions is bounded by the above expression. In n dimensions, it follows that at most

$$O\left(\left(\frac{2w_{\max}(B_0)e^{\bar{\mu}H}}{\varepsilon}\right)^n\right)$$

boxes are created which completes the proof. **Q.E.D.**

B Appendix: More Experiments

We provide some additional experimental data.

The figures below illustrate the trajectories produced by our method and demonstrate how the corresponding end enclosures are obtained.

From these figures, we observe that, in contrast to Lohner's method, our approach mitigates the wrapping effect by explicitly tracking and propagating the boundary of the reachable set. This boundary-oriented strategy prevents excessive over-approximation during enclosure propagation, which explains why our method is able to produce significantly tighter and more accurate end enclosures.

B.1 Time Horizon Sensitivity Analysis

Table 3 summarizes how the output enclosure and computational effort depend on the time horizon T . In general, increasing T tends to enlarge the computed enclosure and to increase the number of initial boxes $\#(\underline{B}_0)$ and run time. The effect can be mild for some problems (e.g., the Quadratic example shows only modest changes in time and $\#(\underline{B}_0)$), but can be drastic for others: Eg2 at $T = 4.0$ requires 56 initial boxes and about 20.36 s, whereas at $T \leq 2.0$ it used at most 10 boxes and under 0.31 s. This indicates that long time propagation may require significantly more subdivision and thus higher computational cost;

B.2 Tolerance Parameter Sensitivity Analysis

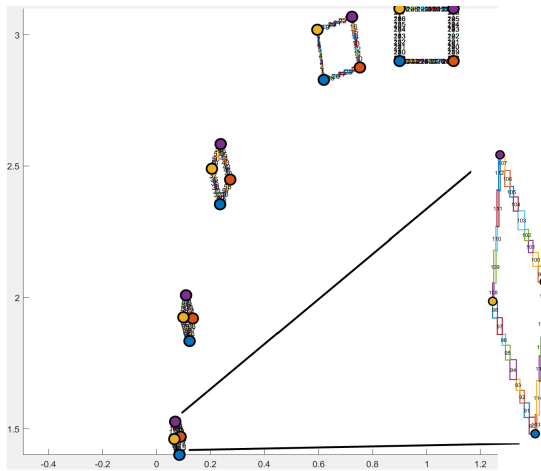
Table 4 analyzes the impact of varying the tolerance parameter ε . As seen in the last two columns of the table, as ε decreases, the width of the end-enclosure decreases (as expected), but the running time increases (as expected).

Case	T	$\text{Box}(\bar{B}_1)$	$\#(\underline{B}_0)$	Time (s)
Eg1	0.5	$[0.152, 0.212] \times [2.170, 2.391]$	8	0.047
	1.0	$[0.062, 0.092] \times [1.395, 1.532]$	8	0.062
	2.0	$[0.064, 0.104] \times [0.553, 0.601]$	8	0.061
	4.0	$[1.052, 1.861] \times [0.136, 0.240]$	12	0.083
Eg2	0.5	$[-2.586, -2.240] \times [0.464, 0.748]$	8	0.044
	1.0	$[-2.3781 - 1.876] \times [0.365, 0.781]$	8	0.086
	2.0	$[-1.783, -1.028] \times [0.607, 1.312]$	10	0.152
	4.0	$[1.351, 2.272] \times [-0.343, 2.470]$	56	2.361
Eg3	0.1	$[-1.311, -1.296] \times [3.986, 4.000]$	8	0.050
	0.4	$[-0.941, -0.933] \times [0.398, 0.419]$	8	0.065
	0.7	$[-0.734, -0.729] \times [-1.519, -1.474]$	8	0.073
	1.0	$[-0.601, -0.598] \times [-6.877, -6.508]$	8	0.082
Quadratic	0.5	$[0.503, 0.680] \times [-0.789, -0.581]$	8	0.018
	1.0	$[0.125, 0.434] \times [-0.743, -0.424]$	8	0.024
	2.0	$[-0.620, 0.069] \times [-0.707, -0.314]$	8	0.061
	4.0	$[-0.888, -0.411] \times [-0.318, 0.828]$	11	0.059

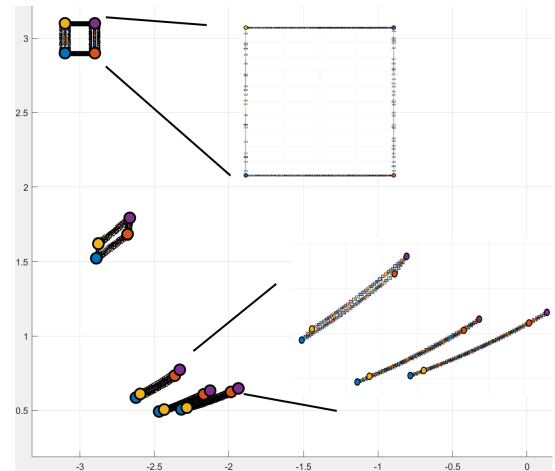
Table 3: Performance variation of the algorithm under different time target T . $\varepsilon = 1.0$.

Case	ε	End-Enclosure B_1	$w_{\max}(B_1)$	Time (s)
Eg1	1.0	$[0.062, 0.092] \times [1.395, 1.532]$	0.137	0.042
	0.5	$[0.062, 0.092] \times [1.395, 1.532]$	0.137	0.042
	0.1	$[0.062, 0.092] \times [1.395, 1.532]$	0.137	0.042
	0.01	$[0.066, 0.089] \times [1.400, 1.527]$	0.126	0.874
Eg2	1.0	$[-2.381, -1.876] \times [0.365, 0.781]$	0.505	0.083
	0.5	$[-2.381, -1.876] \times [0.365, 0.781]$	0.505	0.080
	0.1	$[-2.321, -1.933] \times [0.503, 0.651]$	0.387	0.270
	0.01	$[-2.318, -1.935] \times [0.506, 0.647]$	0.383	3.791
Eg3	1.0	$[-0.601, -0.598] \times [-6.877, -6.508]$	0.369	0.090
	0.5	$[-0.601, -0.598] \times [-6.877, -6.508]$	0.369	0.098
	0.1	$[-0.601, -0.598] \times [-6.872, -6.519]$	0.353	0.293
	0.01	$[-0.601, -0.598] \times [-6.872, -6.519]$	0.352	6.003
Eg4	1.0	$[0.125, 0.434] \times [-0.743, -0.424]$	0.319	0.021
	0.5	$[0.125, 0.434] \times [-0.743, -0.424]$	0.319	0.021
	0.1	$[0.129, 0.432] \times [-0.733, -0.428]$	0.304	0.046
	0.01	$[0.130, 0.432] \times [-0.729, -0.429]$	0.301	0.885
Eg5	1.0	$[1.649, 1.864] \times [0.687, 0.268]$	0.215	0.078
	0.5	$[1.646, 1.866] \times [0.068, 0.268]$	0.220	0.070
	0.1	$[1.678, 1.835] \times [0.070, 0.265]$	0.195	0.169
	0.01	$[1.680, 1.831] \times [0.071, 0.264]$	0.193	2.400
Eg7	1.0	$[-6.976, -6.913] \times [2.986, 3.007] \times [35.104, 35.184]$	0.079	0.647
	0.5	$[-6.976, -6.913] \times [2.986, 3.007] \times [35.104, 35.184]$	0.079	0.647
	0.1	$[-6.976, -6.913] \times [2.986, 3.007] \times [35.104, 35.184]$	0.079	0.647
	0.05	$[-6.976, -6.914] \times [2.987, 3.006] \times [35.105, 35.183]$	0.078	6.083
Eg8	1.0	$[-1.880, -1.588] \times [1.702, 2.039] \times [0.031, 0.035]$	0.337	0.162
	0.5	$[-1.880, -1.588] \times [1.702, 2.039] \times [0.031, 0.035]$	0.337	0.162
	0.1	$[-1.876, -1.591] \times [1.705, 2.036] \times [0.032, 0.035]$	0.331	4.574
	0.05	$[-1.875, -1.592] \times [1.706, 2.036] \times [0.032, 0.035]$	0.329	36.810

Table 4: Performance variation of the algorithm under different tolerance parameters ε .

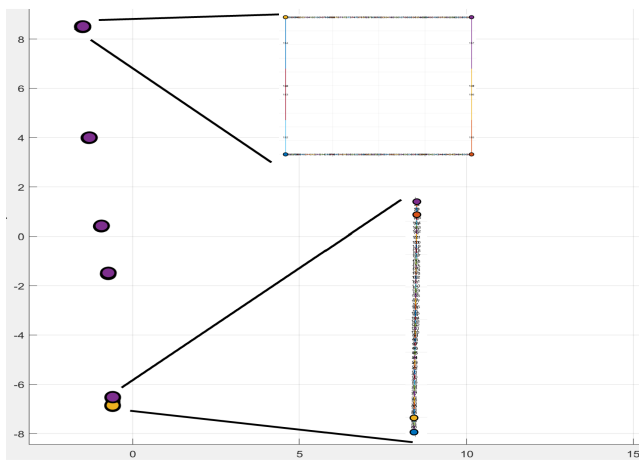


(a) Eg1: Results at $(T = 0, 0.1, 0.4, 0.7, 1.0)$. An enlarged view at $(T = 0.0, 1.0)$ is also shown.

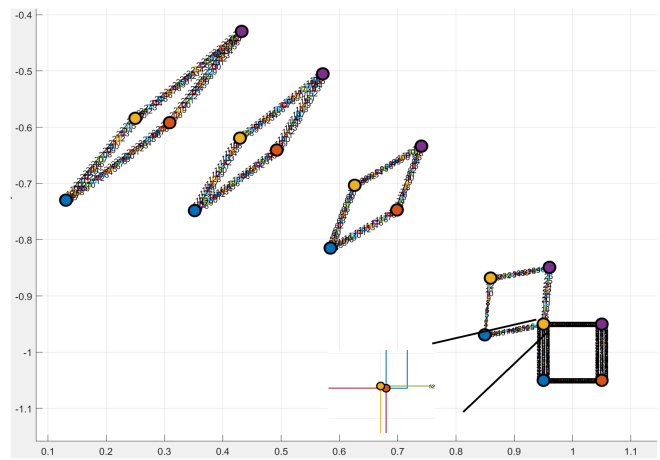


(b) Eg2: Results at $(T = 0, 0.1, 0.4, 0.7, 1.0)$. An enlarged view at $(T = 0.4, 0.7, 1.0)$ is also shown.

Figure 3: Trajectories and end enclosures for Examples Eg1 and Eg2 with $\epsilon = 0.01$.

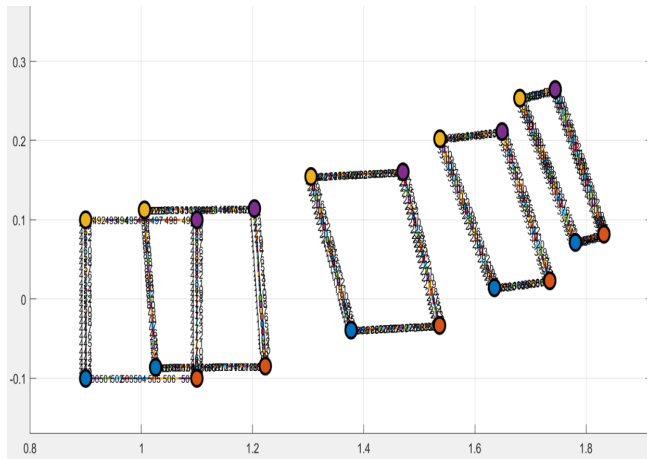


(c) Eg3: Results at $(T = 0, 0.1, 0.4, 0.7, 1.0)$. An enlarged view at $(T = 0.0, 1.0)$ is also shown.

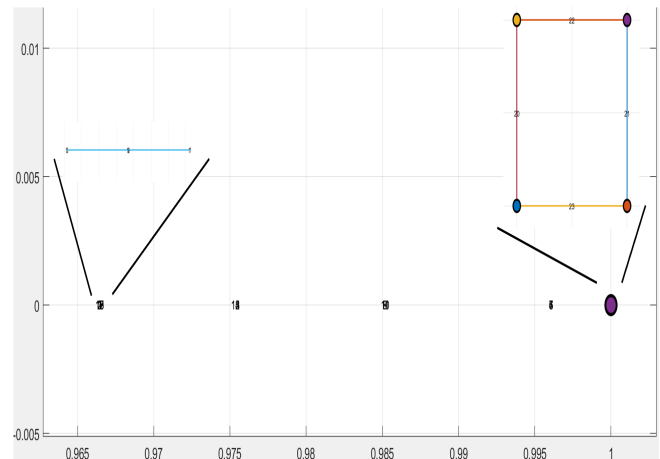


(d) Eg4: Results at $(T = 0, 0.1, 0.4, 0.7, 1.0)$. An enlarged view of the connected component at $(T = 0.0, 0.1)$ is also shown.

Figure 4: Trajectories and end enclosures for Example Eg3 and Eg4 with $\epsilon = 0.01$.



(c) Eg5: Results at $(T = 0, 0.1, 0.4, 0.7, 1.0)$.



(d) Eg6: Results at $(T = 0, 0.1, 0.4, 0.7, 1.0)$. An enlarged view of the connected component at $(T = 0.0, 1.0)$ is also shown.

Figure 5: Trajectories and end enclosures for Example Eg5 and Eg6 with $\varepsilon = 0.01$.